

Precision of finite-difference representation in 3D coordinate-space Hartree-Fock-Bogoliubov calculations

Yue Shi (石跃)^{1,*}

¹*Department of Physics, Harbin Institute of Technology, Harbin 150001, People's Republic of China*

Background The precision of nuclear Hartree-Fock-Bogoliubov (HFB) calculations in coordinate space is limited by box discretization schemes. In particular, for finite-difference (FD) discretization method, the resolution and box size determines the calculation error.

Purpose The current work plans to study the accuracy due to FD approximation to the 3D nuclear HFB problem.

Methods By (1) taking the wave functions solved in harmonic oscillator (HO) basis, (2) representing the HFB problem in coordinate space using FD method, the current work carefully evaluates the error due to box discretization by examining the deviation of the resulted HFB matrix, the total energies in the coordinate space, from those calculated with HO method, the latter of which is free from numerical error within its model configuration. To estimate how the error (given by the box discretization schemes suggested above) accumulates with self-consistent iterations, self-consistent HF and HFB calculations (with two-basis method) has been carried out for doubly magic nuclei, ⁴⁰Ca, ¹³²Sn, and ¹¹⁰Mo. The resulted total energies are compared with those of HO basis, and 3D coordinate space calculations in literatures.

Results The analysis shows that, for grid spacing ≤ 0.6 fm, the off-diagonal elements of the resulted HFB matrix elements (M.E.) are extremely small (< 1 keV). The resulted quasi-particle (q.p.) spectra differ from those of HO calculations by a few keV. Self-consistent HF and HFB calculations within the current FD method with the above box discretization schemes give results similar to those calculations of existing HO basis, and coordinate space method. For the HFB calculations, it is demonstrated that the FD method and the HO method predicted different single-particle spectra, which makes an exact comparison difficult. This makes the analysis of precision at a certain iteration useful.

Conclusions With the described FD approximation to the differential operators, together with the way various densities, and Hamiltonian are constructed in the current work, it can be concluded that for box grid spacing ≤ 0.7 fm, and large enough box size for the studied system, the accuracy of each calculated energy contribution is in the order of a few tens of keV. With this discretization scheme, the number of the calculated M.E. differs from that of HO calculation by $\leq 10\%$ of the total number of the HFB M.E. For the single-particle or q.p. energies, the accuracy is in the order of a few keV. The above conclusions have been verified by performing self-consistent HF, and HFB calculations.

PACS numbers: 21.60.Jz, 21.10.Hw, 21.10.Ky, 21.10.Pc

I. INTRODUCTION

Nuclear density functional theory (DFT) or nuclear self-consistent Hartree-Fock (HF) theory [1] has been successful in describing ground-state (g.s.) properties in nuclei throughout the nuclear chart. After incorporating pairing interaction in the frameworks of Bardeen-Cooper-Schrieff (BCS) or Hartree-Fock-Bogoliubov (HFB) [2], the resulted HF+BCS or HFB theories have become standard models for the description of low-energy phenomena in nuclear physics. In addition, the obtained static solutions provide useful starting points for beyond mean-field calculations [1, 3]. Indeed, static solutions of the g.s. provide starting point for time-dependent analysis which is essential for studying nuclear reaction and fissioning processes [4, 5].

Various mean-field and HFB methods require a fast determination of the solution of Schrödinger equation. In theoretical nuclear physics, two main types of methods exist to solve the non-linear problem. On the one hand, there are methods based on harmonic oscillator (HO) basis expansion [6–16], or, more generally, on the use of an

alytic basis [17]. On the other hand, there are methods that express the w.fs. and operators in coordinate space directly, or using interpolatory techniques [18–32].

Methods based on HO basis possess the following main advantages. (1) Within the Skyrme energy density functional (EDF) theory, the nuclear mean-field Hamiltonian can be evaluated *exactly* without approximation in HO basis [7]; and (2) by limiting the number of HO, the basis expansion methods provide a natural truncation for the problem, which leads to a Hamiltonian matrix with reasonably small size, providing acceptable and tunable precision. Methods using HO basis suffer from strong damping at large space distance from the center of nucleus, so that the precision of these methods may not be guaranteed for systems with large density extension.

Coordinate space methods are complementary when it comes to their numerical properties. Firstly, the representation of w.fs. in coordinate space allows for more extensive w.fs. in real space. Secondly, these methods provide intuitive, and hence, relatively straightforward codes, facilitating further updates. Thirdly, evaluation of quantities on grids could be performed separately, providing excellent parallel scalability, which is particularly suitable for modern super-computers. However, there are two main sources of error related to methods in coordinate space, namely, box size, and grid spacing.

*Electronic address: yueshi@hit.edu.cn

Recently, there has been new efforts in basis optimization for 3D HF(B) calculations, especially using coordinate space [17, 26, 30–35]. Taking advantage of the increasingly larger computing resources involves compromise between the degree of complexity of method used, and the precision that can be accepted for applications at hand. Hence, it is necessary to know the precision of the nuclear HF(B) calculation induced by limited resolution and box size.

Conventionally, one estimates the errors of a self-consistent HF(B) calculation by comparing its calculated results with a presumably more accurate calculation with a lower dimensioned method, allowing for much better resolution in coordinate space [2, 36], the latter being considered close to an exact solution.

However, except for extreme cases [14, 17] where the basis can be made exactly the same, HF(B) calculations of different dimensions can hardly be made identical. This is due to different truncation schemes used for the continuum spectrum, which results in different (quasi-)particle levels retained in respective Fock spaces. This makes strict benchmark calculations extremely difficult to devise, particularly for applications using Cartesian coordinates.

A previous study [37] considered the precision of various techniques including the finite difference (FD) method. In their study, a Woods-Saxon form of mean-field was used to simulate that resulting from an EDF calculation. In the current study, I plan to look into the errors due to box discretization for EDF. In Sec. II, the nuclear DFT is briefly reviewed. The current w.fs., the definition of derivative, and Laplacian operators, and the strategy to quantify precisions will be given at the end of the section. The results of error analysis about FD method will be shown in Sec. III. Then, the self-consistent calculations of Skyrme HF, and HFB using two-basis method will be presented in Sec. IV, before the summary and perspectives, which are shown in Sec. V.

II. THE MODEL

The current work aims at studying the precisions associated with grid spacing and box size in 3D coordinate space HFB calculations. Before presenting the strategy followed to evaluate its precision, in this section, I will recall briefly the formalism of the nuclear Skyrme HFB problem.

A. Quasi-particle states

The q.p. w.fs. are primary inputs for the evaluation of local densities etc. In practice, one uses well-educated initial results from Nilsson, Woods-Saxon, or codes of a lower dimension. In the present work, I plan to estimate the error due to limited resolution of FD procedure by comparing results with those from 3D HO basis.

The w.fs. in coordinate space [Eq. (10) in Ref. [10]] are implemented using the expansion coefficients (A 's and B 's) using HO basis resulting from a converged HFODD (v2.49t) [12] result. Specifically, the upper and lower components of w.fs. in coordinates space read

$$\begin{aligned}\varphi_{\alpha,s=\pm i}^{(1)}(\vec{r}\sigma) &= 2\sigma \sum_{\vec{n}} \psi_{\vec{n},s=\pm i}^*(\vec{r}, -\sigma) A_{\pm, \vec{n}\alpha}^*, \\ \varphi_{\alpha,s=\pm i}^{(2)}(\vec{r}\sigma) &= \sum_{\vec{n}} \psi_{\vec{n},s=\pm i}^*(\vec{r}, \sigma) B_{\pm, \vec{n}\alpha}^*,\end{aligned}\quad (1)$$

where $\psi_{\vec{n},s=\pm i}(\vec{r}\sigma)$ are the HO w.fs. [Eq. (78) in Ref. [7]] in space coordinates [Eq. (76) in Ref. [7]] and $\vec{n} = (n_x, n_y, n_z)$ are the HO quanta numbers in three Cartesian directions. The index $\alpha = 1, \dots, M/2$ numbers eigenstates of HFB equations. The number of q.p. states included in the HFB equations, M , is defined by a cut-off energy E_{cut} .

B. Local densities

Local densities for particle, pairing, kinetic are obtained from q.p. w.fs.,

$$\rho(\vec{r}) = \sum_{\alpha,s=\pm i} \sum_{\sigma=\pm\frac{1}{2}} \left| \varphi_{\alpha,s}^{(2)}(\vec{r}\sigma) \right|^2, \quad (2)$$

$$\tau(\vec{r}) = \sum_{\alpha,s=\pm i} \sum_{\sigma=\pm\frac{1}{2}} \left| \vec{\nabla} \varphi_{\alpha,s}^{(2)}(\vec{r}\sigma) \right|^2, \quad (3)$$

$$\tilde{\rho}(\vec{r}) = -2 \sum_{\alpha} \sum_{\sigma=\pm\frac{1}{2}} \varphi_{\alpha,s=+i}^{(2)}(\vec{r}\sigma) \varphi_{\alpha,s=-i}^{(1)*}(\vec{r}\sigma). \quad (4)$$

For the present applications, spin-orbit density does not appear explicitly. The divergence of spin-orbit density reads

$$\vec{\nabla} \cdot \vec{J} = -i \sum_{\alpha,\sigma,s=\pm i} \left(\vec{\nabla} \varphi_{\alpha,s}^{(2)*}(\vec{r}\sigma) \right) \cdot \left(\vec{\nabla} \times \vec{\sigma} \right) \varphi_{\alpha,s}^{(2)}(\vec{r}\sigma). \quad (5)$$

To this point the index (q) denoting neutron (n) and proton (p) has been ignored for simplicity.

C. The energy-density functional

For Skyrme-HFB calculation, the total energy E of a nucleus is the sum of kinetic, Skyrme, pairing, and Coulomb terms:

$$\begin{aligned}E &= E_{\text{Kin+c.m.}} + E_{\text{Skyrme}} + E_{\text{pair}} + E_{\text{Coul}} \\ &= \int d^3\vec{r} [\mathcal{K}(\vec{r}) + \mathcal{E}_{\text{Skyrme}}(\vec{r}) \\ &\quad + \mathcal{E}_{\text{pair}}(\vec{r}) + \mathcal{E}_{\text{Coul}}(\vec{r})].\end{aligned}\quad (6)$$

The derivation of the total energy has been presented in detail in Refs. [38, 39] for the HF case, and in Ref. [2] for the HFB case.

In Eq. (6), the kinetic energies of both neutron and proton are given by

$$\mathcal{K} = \frac{\hbar^2}{2m} \tau \left(1 - \frac{1}{A} \right), \quad (7)$$

where the factor in between parentheses takes into account the one-body part of center-of-mass correction [36]. As the current work only considers even-even nuclei, the Skyrme part of the EDF is time even. The energy density functional reads

$$\begin{aligned} \mathcal{E}_{\text{Skyrme}} = & \frac{b_0}{2} \rho^2 - \frac{b'_0}{2} \sum_q \rho_q^2 + \frac{b_3}{3} \rho^{\alpha+2} - \frac{b'_3}{3} \rho^\alpha \sum_q \rho_q^2 \\ & + b_1 (\rho\tau - j^2) - b'_1 \sum_q (\rho_q \tau_q - j_q^2) \\ & - \frac{b_2}{2} \rho \nabla^2 \rho + \frac{b'_2}{2} \sum_q \rho_q \nabla^2 \rho_q \\ & - b_4 \rho \vec{\nabla} \cdot \vec{J} - b'_4 \sum_q \rho_q (\vec{\nabla} \cdot \vec{J}_q). \end{aligned} \quad (8)$$

The index q denotes neutron and proton. The densities without index indicate the sum of neutron and proton densities. The time-odd current densities (\vec{j}, \vec{j}_q) are identically zero for the current time-independent study.

The pairing density is [22]

$$\mathcal{E}_{\text{pair}} = \sum_q \frac{V_0^q}{4} \tilde{\rho}_q^2(\vec{r}) f(\vec{r}). \quad (9)$$

Volume pairing is used in the current study, so that $f(\vec{r}) = 1$.

D. HFB mean-fields

Varying the total energy Eq. (6) with respect to ρ and $\tilde{\rho}$ one obtains the HFB equation [2, 3]

$$[\mathcal{W}, \mathcal{R}] = 0, \quad (10)$$

where

$$\mathcal{W} = \begin{pmatrix} h - \lambda & \tilde{h} \\ \tilde{h} & -h + \lambda \end{pmatrix}, \quad (11)$$

and

$$\mathcal{R} = \begin{pmatrix} \rho & \tilde{\rho} \\ \tilde{\rho} & \delta(\vec{r} - \vec{r}') \delta_{\sigma\sigma'} - \rho \end{pmatrix}. \quad (12)$$

In Eq. (11), the Lagrange multiplier λ guarantees $\int d^3\vec{r} \sum_\sigma \rho(\vec{r}\sigma, \vec{r}\sigma)$ to be equal to the proton or neutron number.

The mean-fields and densities appearing in Eqs. (10,11,12) are not necessarily local [2, 40]. But due to the zero-range of Skyrme force used in the

current work, the densities in Eq. (12) can be expressed using only local particle and pairing densities [2, 38]

$$\rho(\vec{r}\sigma, \vec{r}'\sigma') = \frac{1}{2} \rho(\vec{r}) \delta(\vec{r} - \vec{r}') \delta_{\sigma\sigma'}, \quad (13)$$

$$\tilde{\rho}(\vec{r}\sigma, \vec{r}'\sigma') = \frac{1}{2} \tilde{\rho}(\vec{r}) \delta(\vec{r} - \vec{r}') \delta_{\sigma\sigma'}, \quad (14)$$

where the time-odd parts have been ignored as they identically vanish in a static study. In Eq. (11) the mean-field Hamiltonian (q distinguishing n , and p) reads

$$\begin{aligned} h_q(\vec{r}\sigma, \vec{r}'\sigma') = & \left[-\vec{\nabla} \cdot \frac{\hbar^2}{2m_q^*} \vec{\nabla} + U_q \right] \delta(\vec{r} - \vec{r}') \delta_{\sigma\sigma'} \\ & - \left[i\vec{B}_q (\vec{\nabla} \times \vec{\sigma}) \right]_{\sigma\sigma'} \delta(\vec{r} - \vec{r}'), \end{aligned} \quad (15)$$

where the effective mass is defined by

$$\frac{\hbar^2}{2m_q^*} = \frac{\hbar^2}{2m_q} + b_1 \rho - b'_1 \rho_q, \quad (16)$$

and the effective spin density

$$\vec{B}_q = b_4 \vec{\nabla} \rho + b'_4 \vec{\nabla} \rho_q. \quad (17)$$

The nuclear potential due to Skyrme force reads

$$\begin{aligned} U_q = & b_0 \rho - b'_0 \rho_q + b_1 \tau - b'_1 \tau_q \\ & + \frac{b_3}{3} (\alpha + 2) \rho^{\alpha+1} - \frac{b'_3}{3} \left[\alpha \rho^{\alpha-1} \sum_q (\rho_q^2 + 2\rho^\alpha \rho_q) \right] \\ & - b_4 \vec{\nabla} \cdot \vec{J} - b'_4 \vec{\nabla} \cdot \vec{J}_q \\ & - b_2 \nabla^2 \rho + b'_2 \nabla^2 \rho_q. \end{aligned} \quad (18)$$

Note that the Hamiltonian in Eq. (15) is a 2×2 matrix in σ -space. The pairing mean-field, which is diagonal in σ -space, reads

$$\tilde{h}_q(\vec{r}\sigma, \vec{r}'\sigma') = \frac{1}{2} V_0^q \tilde{\rho}_q(\vec{r}) f(\vec{r}) \delta(\vec{r} - \vec{r}') \delta_{\sigma\sigma'}. \quad (19)$$

E. Coulomb potential and energy

The protons potential includes Coulomb contributions. Its direct part is obtained by solving the electrostatic Poisson equation

$$\Delta U_{\text{Coul}}^{(\text{Dir.})}(\vec{r}) = -4\pi e^2 \rho_p(\vec{r}). \quad (20)$$

The boundary conditions need to be imposed according to

$$U(\vec{r}) = \frac{e^2 Z}{r} + e^2 \frac{\langle \hat{Q}_{20} \rangle Y_{20}(\vec{r}) + \langle \hat{Q}_{22} \rangle \mathcal{R} Y_{22}(\vec{r})}{r^3}, \quad (21)$$

where the multiple moments \hat{Q}_{20} and \hat{Q}_{22} are defined by using the spherical harmonics, $\hat{Q}_{\lambda\mu} = r^\lambda Y_{\lambda\mu}$, specifically,

$$\hat{Q}_{20} = \sqrt{\frac{5}{16\pi}} (2z^2 - x^2 - y^2), \quad (22)$$

$$\hat{Q}_{22} = \sqrt{\frac{15}{32\pi}} (x^2 - y^2). \quad (23)$$

For details, see Ref. [30].

The exchange part of the Coulomb potential is approximated by Slater approximation. Its contribution to the Coulomb potential is

$$U_{\text{Coul}}^{(\text{Exc.})} = -e^2 \left(\frac{3}{\pi} \right)^{1/3} [\rho_p(\vec{r})]^{1/3}. \quad (24)$$

The contributions of direct and exchange Coulomb energies are,

$$E_{\text{Coul}} = E_{\text{Coul}}^{(\text{Dir.})} + E_{\text{Coul}}^{(\text{Exc.})}, \quad (25)$$

where

$$E_{\text{Coul}}^{(\text{Dir.})} = \frac{1}{2} \int d\vec{r} U_{\text{Coul}}^{(\text{Dir.})} \rho_p(\vec{r}), \quad (26)$$

and

$$E_{\text{Coul}}^{(\text{Exc.})} = -\frac{3e^2}{4} \left(\frac{3}{\pi} \right)^{1/3} \int d\vec{r} \rho_p^{4/3}(\vec{r}). \quad (27)$$

F. Finite-difference discretization of q.p. states and operators

The current work adopts FD discretization in coordinate space. Though FD are known to be inferior in terms of precision compared to Fourier transformations or spline techniques [37], it provides reasonable balance between cost and precision. In computational intense simulations such as TDHF, and 3D HFB, FD is still widely used [41, 42]. It is the purpose of the present work to examine (1) that to what extend a simple, and efficient FD method could approach a self-consistent HF(B) problem, and (2) its accuracy.

Figure 1 illustrates how the cubic and uniformly placed grid points are defined by grid spacings, $\Delta x, y, z$ (in fm), and $N_{\text{max}}^{x,y,z}$ which numerate the outer-most grid point in each axis. The box size is thus $(2\Delta x \cdot N_{\text{max}}^x) \times (2\Delta y \cdot N_{\text{max}}^y) \times (2\Delta z \cdot N_{\text{max}}^z)$ (fm³). No symmetry has been enforced in the current work.

The derivative, and Laplacian operations are evaluated on grids using seven-, and nine-point formula, respectively [43]. These choices have been proven to be stable, and reasonably accurate within FD method from a few groups in different applications [18, 20, 37, 42, 44]. The current work examines precisions of the same setup (seven-, and nine-point formula) by comparing the results with HFODD while varying the discretization schemes, at a fixed iteration. Note that, even though the operators are constructed the same way, how the Hamiltonian is calculated numerically may give rise to errors. For example, two different methods to construct kinetic density (3) result in the kinetic energies (7) being different by a few MeV, as shown table I.

The integrations are performed using the trapezoidal rule [45]. Specifically, the summed value at the center of

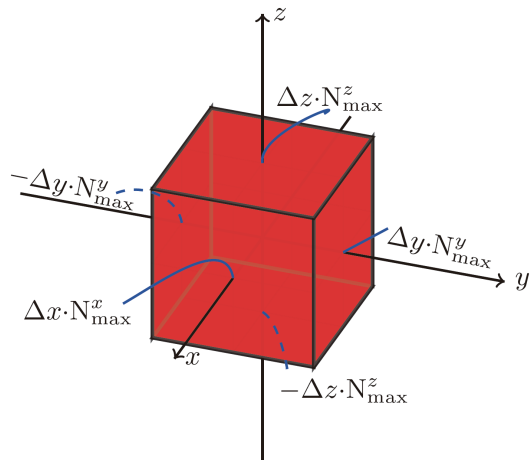


FIG. 1: Schematic figure depicting grid spacings, Δx , Δy , and Δz , and box size (through N_{max}^x , N_{max}^y , and N_{max}^z) in coordinate space method.

each cell is evaluated by averaging values at the eight surrounding corners [46]. This procedure differs from other existing FD implementations, where rectangular rules are used [18, 20, 41, 42, 44]. Representing the problem *on* the grid points instead of the center allows for more elaborate interpolatory and extrapolatory methods [45].

The error associated with this non-conventional way of integration can be seen in Sec. III, where the orthonormality condition (30) of the w.fs., which are imported from HFODD results, are fulfilled to high precision. The precision of the integration procedure can also be assessed from table I, where the density-related energies in the Skyrme terms (E_{ρ^2} , $E_{\rho^2+\alpha}$) are rather close to that of the HFODD values even for the most coarse discretization scheme.

III. QUANTIFICATION OF ERRORS DUE TO THE FD APPROACH TO THE HFB PROBLEM

To assess the precision of given resolution-box-size combination, I will take the q.p. w.f. (1) resulting from 3D HFB code HFODD [7–14]. The Skyrme force parameter SkM* [2] has been used. Volume pairing is used with both proton and neutron pairing strengths of 200 MeV fm⁻³.

Defining

$$\phi_\alpha(\vec{r}\sigma) = \begin{pmatrix} \varphi_{\alpha,s=-i}^{(1)}(\vec{r}\sigma) \\ \varphi_{\alpha,s=-i}^{(2)}(\vec{r}\sigma) \end{pmatrix}, \quad (28)$$

one obtains the HFB matrix (11) with matrix elements (M.E.)

$$h_{\alpha\beta} \equiv \sum_{\sigma\sigma'} \iint d^3\vec{r} d^3\vec{r}' \phi_\alpha^+(\vec{r}\sigma) \mathcal{H} \phi_\beta(\vec{r}'\sigma'). \quad (29)$$

In the present case, the w.fs. in Eq. (28) is a self-consistent solution of the HFB problem in HO basis. Only states having $s = -i$ are chosen so that the diagonal M.E. $h_{\alpha\alpha}$ are all positive, whereas the spectra for $s = +i$ are $-h_{\alpha\alpha}$ [10]. In this work, it has been checked that the orthonormality condition

$$\sum_{\sigma} \int d^3\vec{r} \phi_{\alpha}^{\dagger}(\vec{r}\sigma) \phi_{\beta}(\vec{r}\sigma) = \delta_{\alpha\beta}, \quad (30)$$

is fulfilled up to high precision.

Ideally, if the FD representation is precise, the matrix $h_{\alpha\beta}$ should be diagonalized as they are resulted from the self-consistent HFB problem in HO basis. The deviation of HFB equation (29) from diagonalization reflects the error of FD representation. The current work measures the round-off errors by comparing the deviation of Eq. (29) from a diagonalized matrix $h_{\alpha\beta}^{\text{HO}}$, which is from HFODD calculation.

Figure 2 shows the number of off-diagonal M.E. (29) that lies in the intervals $[0, 0.001)$, $[0.001, 0.01)$, $[0.01, 0.1)$, and $[0.1, 0.2)$ for discretizing schemes listed in table I. For both 300 and 680 HO basis, there is a dominance of M.E. with values < 0.001 MeV, especially for ‘E-G’. With decreasing grid spacing (from ‘A’ to ‘G’), there is a continuous increase of M.E. with values < 0.001 MeV. To better evaluate the quality that these discretization schemes offer, one needs to have a criteria. In the following discussions, if the number of M.E., whose values are ≥ 10 keV, is lower than 10^3 , which is less than 10% of the total number of the off-diagonal M.E., then the corresponding discretizing scheme is considered to be offering reasonably accurate results. With this criteria in mind, one may find that the HFB matrix is reasonably diagonalized for grid spacings smaller than 0.7 fm (‘C-G’ schemes). From figure 2, it can be seen that, for grid spacings of 0.5-0.6 fm, there are 10^2 - 10^3 M.E. with values between 1-10 keV. This means that a grid spacing of 0.5-0.6 fm provides precision on the s.p. or q.p. levels of the order of 1-10 keV.

TABLE I: Definition of box size and spacings used in the calculations.

Label	A	B	C	D	E	F	G
$\Delta x, y, z$ (fm)	1.0	0.9	0.8	0.7	0.6	0.5	0.4
$N_{\text{max}}^{x,y,z}$	14	14	16	18	22	26	32
Box size (fm)	28.0	25.2	25.6	25.2	26.4	26	25.6

Figure 3 shows the number of off-diagonal M.E. for grid spacing of 1.0 fm as a function of box size. The distribution of M.E. is varying for small box sizes (≤ 24 fm), and stabilizes for box size larger than 24 fm. For a basis number of $M=680$ (lower panel), the box size at which the distribution stabilizes is slightly larger than that of $M=300$ (upper panel). The number of large M.E. can only be reduced by decreasing the grid spacings. These are expected for medium heavy nuclei from studies based on HO basis.

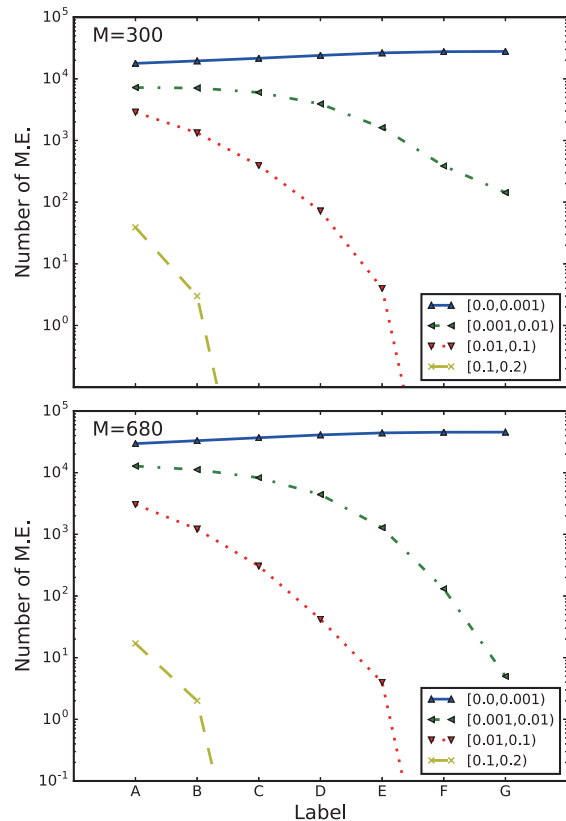


FIG. 2: Number of off-diagonal M.E. in the intervals of $[0, 0.001)$, $[0.001, 0.01)$, $[0.01, 0.1)$, and $[0.1, 0.2)$ for discretizations ‘A–G’ listed in table I.

Figure 4 displays the occupation probabilities

$$v_{\alpha}^2 = \sum_{\sigma} \int d^3\vec{r} \left| \varphi_{\alpha, s=-i}^{(2)}(\vec{r}\sigma) \right|^2, \quad (31)$$

against the q.p. energies obtained with HFODD ($M=300$). For discretization schemes ‘A-F’, the diagonal M.E. of $h_{\alpha\alpha}$ for $\alpha = 1, \dots, M/2$ are used. It can be seen that the q.p. spectra for HFODD, and ‘A-F’ overlap with each other, and one could not distinguish them from one another. In general, from scheme to scheme, the differences of q.p. energies are mostly under 1 keV throughout the spectra. The ‘F’ discretization scheme spectrum is almost identical with the one calculated with HFODD. This is consistent with the situation shown in figure 2, where the error due to finite grid spacing is $\sim 0.001 - 0.01$ MeV for grid spacings ≤ 0.6 fm.

Apart from the errors of s.p., or q.p. levels, which is associated with the approximated treatment of s.p., or q.p. Hamiltonian, another important source of error is due to the evaluation of integral quantities such as total energies. In table II, I list the total energy of ^{110}Mo and its decomposition into various terms, calculations are done with FD method for discretization schemes listed in table I. The results are compared with those of HFODD calculations with $M=300$ which corresponds to $N=11$.

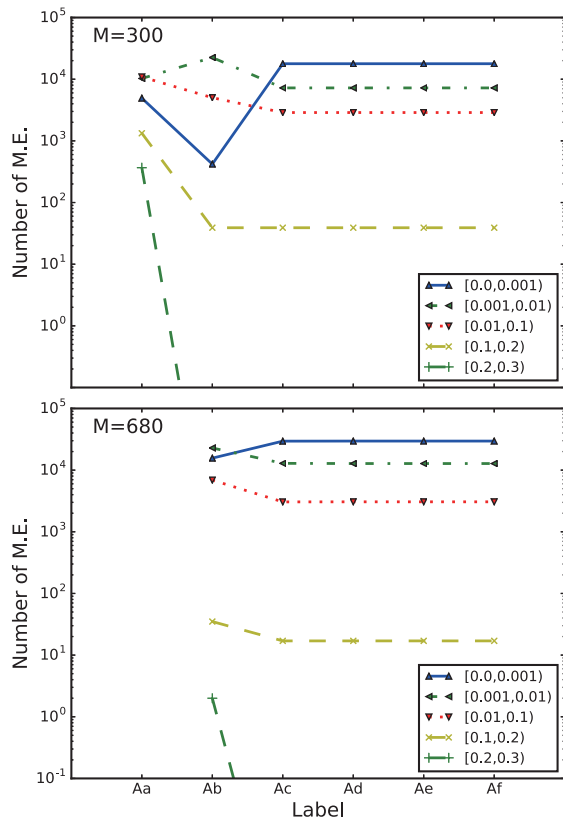


FIG. 3: Number of off-diagonal M.E. in the intervals $[0, 0.001)$, $[0.001, 0.01)$, $[0.01, 0.1)$, $[0.1, 0.2)$, and $[0.2, 0.3)$. Labels ‘Aa’ to ‘Af’ denote results with box sizes ranging from 16.0 to 36.0 fm at equal distance.

For terms containing kinetic densities in Skyrme and kinetic (7) energies, a second row has been added, where the kinetic densities, τ , is evaluated with Laplacian operator by using [32]

$$\tau(\vec{r}) = \frac{1}{2} \Delta \rho(\vec{r}) - \text{Re} \left(\sum_{\alpha, s = \pm i} \sum_{\sigma = \pm \frac{1}{2}} \phi_{\alpha, s}^{(2)*}(\vec{r}\sigma) \Delta \phi_{\alpha, s}^{(2)}(\vec{r}\sigma) \right). \quad (32)$$

As expected, the energies converge towards the HFODD results with decreasing grid spacings. It is interesting to note that, the method used to evaluate the kinetic density in FD method, using (3) or (32), impacts the speed of convergence. With Eq. (3), for ‘G’ configuration, the total energy differs from the HFODD result by ≤ 200 keV. Using Eq. (32), the energies converge to HFODD result at a much larger grid spacing (0.7 fm) than the results given by Eq. (3).

In the following discussions, a guideline will be defined to assess these discretization schemes: if an energy calculated with certain box discretization differs from the value calculated with HFODD by ≤ 100 keV, then the respective discretizing scheme is considered to be reasonably accurate. It is then noticed that the terms containing differential operations ($E_{\text{Kin+c.m.}}$, $E_{\rho\tau}$,

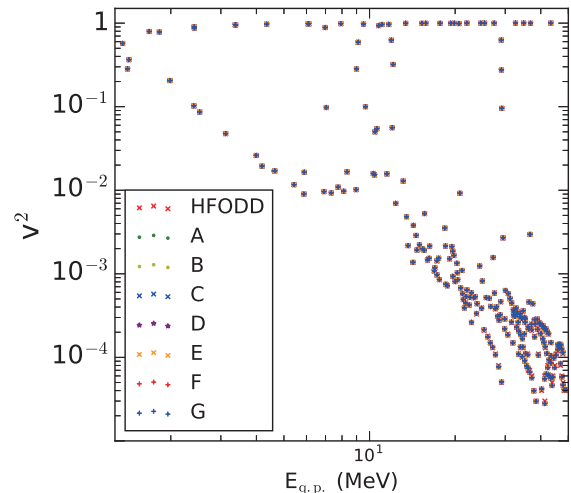


FIG. 4: Occupation probabilities (31) as a function of quasi-particle energies (in MeV), resulted from HFODD ($M=300$) and FD (‘A-F’ configurations in Table. I) calculations.

$E_{\rho\Delta\rho}$, and $E_{\rho\nabla J}$) shows lowered precision for discretization schemes ‘C’. In particular, according to the values of $E_{\text{Kin+c.m.}}$, one may find that ‘D-G’ configurations with $\Delta x, y, z \leq 0.7$ fm provide much better approximation than that of ‘C’. This situation contrasts with that shown in figures 2, and 3, where the discretization scheme ‘C’ already provide rather good accuracy on the q.p. levels, with majority of the M.E. being smaller than 10 keV.

IV. SELF-CONSISTENT CALCULATIONS

A. self-consistent HF calculations

In this section, I examine the results when self-consistency has been achieved, by comparing results calculated in the current work with that of HFODD. As has been noted in the introduction, there are ambiguities for calculations represented in different dimensions. This is due to different truncation schemes. These differences make a stringent benchmark calculation difficult. HF calculations for light doubly magic nuclei are probably most suited to perform benchmark calculations, where the differences in s.p. space are minimized.

I perform self-consistent HF calculations for a well defined light nucleus ^{40}Ca , and a heavier nucleus ^{132}Sn . The results are tabulated in table III. Although being fundamentally different in the pairing treatment, the sources of error due to box discretization for both methods are rather similar. This is because neither the pairing density (14), nor pairing Hamiltonian (19) contain any differential operation, which is the main source of error of FD method.

The self-consistent HF problem is solved by updating w.fs. using an imaginary time step method [47], which provides stable converged solution. Iteration is termi-

TABLE II: Total energy of ^{110}Mo and its decompositions into $E_{\text{Kin+c.m.}}$ (7) and various terms in E_{Skyrme} , with HFODD code (M=300) and FD procedure with various box configurations in table I. All values in the table are in MeV.

	C	D	E	F	G	HFODD
$E_{\text{Kin+c.m.}}$	2004.509 2010.523	2007.762 2010.606	2009.459 2010.639	2010.240 2010.650	2010.542 2010.653	2010.654
$E_{\text{Coul}}^{(\text{Dir.})}$	266.908	266.903	266.902	266.899	266.897	266.908
$E_{\text{Coul}}^{(\text{Exc.})}$	-15.744	-15.744	-15.744	-15.744	-15.744	-15.744
E_{ρ^2}	-12266.985	-12266.985	-12266.985	-12266.985	-12266.985	-12266.984
$E_{\rho\tau}$	367.613 368.964	368.345 368.988	368.729 368.997	368.907 369.001	368.976 369.002	369.002
$E_{\rho^2+\alpha}$	8600.091	8600.091	8600.091	8600.091	8600.091	8600.090
$E_{\rho\Delta\rho}$	193.189	193.209	193.218	193.221	193.222	193.222
$E_{\rho\nabla J}$	-73.778	-73.935	-74.018	-74.056	-74.071	-74.077
E_{pair}	-3.816	-3.816	-3.816	-3.816	-3.816	-3.816
E_{Skyrme}	-3179.870 -3178.519	-3179.275 -3178.632	-3178.965 -3178.697	-3178.822 -3178.728	-3178.767 -3178.741	-3178.747
E_{Total}	-928.014 -920.649	-924.172 -920.684	-922.164 -920.716	-921.243 -920.739	-920.888 -920.751	-920.745

nated when sum of the dispersions of the single particle energies, $\frac{1}{A} \sum_{\alpha} [(h^2)_{\alpha\alpha} - (h_{\alpha\alpha})^2] < 1.0 \times 10^{-5}$ for ten iterations. Note, that the h here is the s.p. Hamiltonian which appears in Eq. (11). With this criteria of convergence, the difference of total energy, between the current iteration compared to the previous one, is only 10^{-8} of the total energy of the current iteration. For the solution of the Coulomb potential, I follow the procedure described in Refs. [30, 44].

In fact, the current part of the implemented code, which solves the nuclear self-consistent HF problem, differs from those in Refs. [30, 44] mainly by the following items:

- (1) I do not assume any symmetry in coordinate space, although time-reversal symmetry is present.
- (2) I do not use any interpolatory techniques to maintain the simplicity, flexibility, and short execution time of FD method.

The results are compared with the HFODD calculations with M=969 (N=18). The box sizes and grid spacings are chosen to be close to the ‘E-F’ configurations in table I. It can be seen that the total energies of ^{40}Ca are rather close to the results with HFODD. For the heavier system, ^{132}Sn , the FD results are 500 keV lower than the HFODD calculation. This is consistent with previous results shown in Ref. [26]. It is comforting to see that the total energies shown in table III are the same, within a few tens of keV, as the total energies in tables 4, and 5 in Ref. [30].

B. self-consistent HFB calculations

To solve the HFB problem in coordinate space, a standard method is the two-basis method devised in

TABLE III: Calculated energies for ^{40}Ca and ^{132}Sn with box discretization schemes of $(\Delta x, x)=(0.625, 30)$ fm (denoted with ‘O’), $(0.5357, 30)$ fm (‘P’). The last column lists results from HFODD calculation with basis size of M=969. All values given are in MeV.

	O	P	HFODD
^{40}Ca			
E_{tot}	-344.259	-344.260	-344.251
$E_{\text{Kin.+c.m.}}$	633.732	633.686	644.959
$E_{\text{Coul}}^{(\text{Dir.})}$	79.502	79.500	79.616
$E_{\text{Coul}}^{(\text{Exc.})}$	-7.478	-7.477	-7.489
E_{Skyrme}	-1050.0146	-1049.969	-1051.336
^{132}Sn			
E_{tot}	-1103.508	-1103.535	-1102.935
$E_{\text{Kin.+c.m.}}$	2442.970	2442.784	2444.223
$E_{\text{Coul}}^{(\text{Dir.})}$	359.857	359.837	360.169
$E_{\text{Coul}}^{(\text{Exc.})}$	-18.806	-18.805	-18.820
E_{Skyrme}	-3887.529	-3887.351	-3888.507

Ref. [19]. The two-basis method is advantageous in two ways. Firstly, it is possible to reduce the dimension of the problem to the s.p. space that is below a cutoff energy, $\epsilon \leq \bar{\epsilon}_{\text{max}}$. This allows for reducing by half the dimension of the HFB matrix that is needed to be diagonalized in the standard HFB methods. In the imaginary-time-evolution methods [19], using two-basis method is even more beneficial as one works with the s.p. states as basis and the largest dimension of the problem is considerably lower than the standard HFB methods. The price that one needs to pay is that, the calculation of M.E. is numerically expensive. But the calculation of these M.E., which is shown in Eq. (10), can be conveniently parallelized in multi-node computers. Secondly, the two-basis method, using s.p. states as basis, avoids problems related to the cutoff in the quasi-particle (q.p.) space [48].

TABLE IV: Calculated energies for ^{110}Mo with the HFB code developed in this work (box discretization schemes of $(\Delta x, x)=(0.725, 34.8)$ fm). The results are compared with that of HFODD calculations with basis size of $M=969$. The oscillator constant is $0.4975890 \text{ fm}^{-1}$. The parameterization is SKM*, with $\hbar^2/2m=20.73 \text{ MeV fm}^2$. For ‘b’, the cutoff energy on s.p. levels is 10 MeV; for ‘a’ and HFODD, the s.p. energy cutoff is 20 MeV; the pairing strengths are $V_0=-250 \text{ MeV fm}^{-3}$ for both protons and neutrons. Proton pairing vanishes for all cases.

	a	b	HFODD
E_{tot} (MeV)	-921.954	-922.004	-921.846
$E_{\text{Kin.}+\text{c.m.}}$ (MeV)	2005.555	2005.360	2003.932
$E_{\text{Coul}}^{(\text{Dir.})}$ (MeV)	266.771	266.774	266.908
$E_{\text{Coul}}^{(\text{Exc.})}$ (MeV)	-15.740	-15.740	-15.751
E_{Skyrme} (MeV)	-3176.694	-3177.047	-3175.965
E_{pair} (MeV)	-1.846	-1.351	-0.970
Δ^n (MeV)	0.469	0.403	0.336
λ^n (MeV)	-5.470	-5.476	-5.507
Q_{20}^{total} (b)	298.80	298.45	295.20
$ Q_{22}^{\text{total}} $ (b)	75.46	75.55	82.20

In this section, I summarize the key points of the two-basis procedure before showing the results. For details, the reader is referred to Ref. [19]. The method uses s.p. states of the mean-field Hamiltonian (15) as basis to solve the HFB problem (10). The procedure consists of two steps. The outer routine proceeds as in the HF problem shown in section IV A. The inner routine includes the following procedures at each imaginary step: the HFB (10) M.E. are calculated in the s.p. states; the canonical transformation is obtained afterwards; and finally the densities in coordinate space is constructed. Note, that the Lagrangian multiplier is updated in the inner routine.

In table IV, the calculated properties of triaxial nucleus ^{110}Mo are shown. The energies are compared with that of HFODD with basis number $M=969$. It can be seen that the total energies are the same up to a few hundreds of keV. This is acceptable, if one notices that the two methods differ through the basis used, one being in coordinate space, the other being in HO basis (HFODD). The quadrupole moments listed in table IV are defined in Eqs. (22,23).

From table IV, one can see that although total energies are rather close, each contribution differs. The pairing energies differ by as large as $\sim 1 \text{ MeV}$ for ‘a’, and HFODD. This situation seems to be similar to that in Ref. [13], where the two-basis method gives pairing energies $\sim 1.0 \text{ MeV}$ different from the standard HFB results. Both of their calculations are made with same HO basis.

Moreover, the spectrum for $\epsilon_n \geq 0 \text{ MeV}$ are not the same in the present calculations and that of HFODD. Specifically, in our calculation the number of levels included in the HFB calculation ($\epsilon_n \leq 20 \text{ MeV}$) is 180, whereas in HFODD, the number is 140. This is expected, since in the current work, the w.fs. are expressed in real space, the discretization of the continuum spectrum of

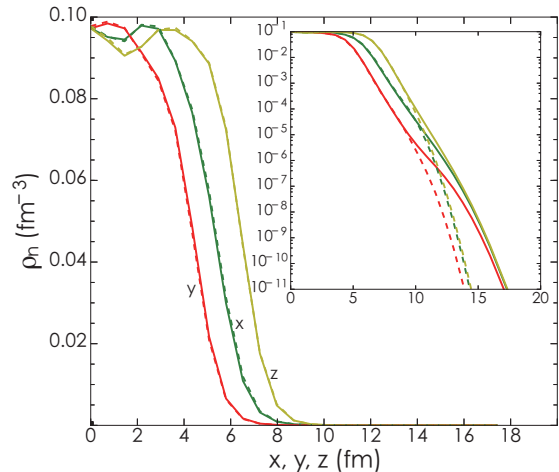


FIG. 5: Neutron density profiles along x-, y-, and z-axis for ^{110}Mo (result ‘a’ in table IV). The dashed lines are respective HFODD results ($M=680$).

neutrons is certainly different from the HFODD calculations, where the w.fs. are expanded in the HO basis.

Table IV column ‘b’ shows the results with smaller s.p. energy cutoff, $\bar{\epsilon}_{\text{max}} \leq 10 \text{ MeV}$. It can be seen that the pairing properties are now closer to the results of HFODD. This comparison should not be considered to be an effort to make these two methods identical, as the two methods discretize the continuum in the q.p. spectra in two different ways. Hence, the two HFB methods can *not* be identical, and the energy differences between the two methods could not be considered to be due to a lack of precision from either of the methods. It has to be noted that existing realistic applications [20, 21] of the two-basis method use an energy cutoff of 5 MeV above Fermi surface, which is smaller than the current calculations.

Figure 5 shows density values along x-, y-, and z-axis. It can be seen that the HO results (dashed lines) display characteristic damping at $r \approx 10 \text{ fm}$, whereas the density values with coordinate-space code (solid lines) start to decrease at the border of the box ($r = 17.4 \text{ fm}$). Another observation is that the lack of resolution seems to have larger influence at the center of the nucleus. It can be expected that a box setup with more grid density at the center part would increase precision.

V. SUMMARY

To summarize, the current work studied the precision of finite difference (FD) approximations to the three-dimensional (3D) nuclear Hartree-Fock-Bogoliubov (HFB) problem. To single out the error due to basis discretization, I first performed the HFB calculations in 3D harmonic oscillator (HO) in Cartesian coordinates. The obtained wave functions (w.fs.), together with the derivative and Laplacian operators, were then constructed us-

ing FD method. The error was evaluated by examining the deviation of the obtained HFB equation from a diagonalized one, the deviation of the diagonal matrix elements (M.E.) from those resulted from HO basis, as well as the deviation of the total energies from the results calculated with HO basis method.

It is surprising to note that the HFB matrix resulted from FD method is rather close to the one obtained from HO basis, with a grid spacing of 0.8 fm. Specifically, in the obtained HFB matrix, the number of off-diagonal M.E. that are smaller than 0.1 MeV dominates, whereas the diagonal M.E. have values in the order of several to a few tens of keV. The number of non-zero M.E. decrease rapidly with decreasing grid spacing. The error of q.p. levels is rather small: the difference for the spectra, with varying grid spacing, is only a few keV in general. Total energy was calculated to be only ~ 10 keV different from the one resulted from HO basis at $\Delta x=0.6$ fm. For a discretizing space of 0.7 fm, each contribution of the energy difference with respect to the HO result was lower than 100 keV. This provided acceptable precision for the FD method in the current work. Results with larger grid spacings ($\Delta x \leq 0.8$ fm) exhibited an important loss of accuracy. For evaluation of kinetic energy, the importance using Eq. (32) instead of Eq. (3) was emphasized.

The effect of self-consistency was studied by perform-

ing self-consistent HF calculations for doubly magic nuclei, ^{40}Ca , and ^{132}Sn . The results for grid spacing ~ 0.6 fm were consistent with results obtained with HO basis method, and existing similar 3D coordinate space methods. In addition, the self-consistent HFB calculations, in the two-basis method, for triaxially deformed nucleus ^{110}Mo were performed. The results were compared with those from HFODD. It was demonstrated that the spectra for the two models (coordinate space and HO) differ for positive energy values.

Acknowledgments

Useful discussions with M. Bender, D.L. Fang, Y. Gao, M. Kortelainen, J.C. Pei, J. Toivanen, and C.X. Yuan are gratefully acknowledged. I thank N. Michel, and W. Nazarewicz for their careful reading of the manuscript and useful comments. The current work is supported by National Natural Science Foundation of China (Grant No. 11705038). I thank the HPC Studio at Physics Department of Harbin Institute of Technology for computing resources allocated through INSPUR-HPC@PHY.HIT.

-
- [1] M. Bender, P.-H. Heenen, and P.-G. Reinhard, *Rev. Mod. Phys.* **75**, 121 (2003).
- [2] J. Dobaczewski, H. Flocard, and J. Treiner, *Nuclear Physics A* **422**, 103 (1984).
- [3] P. Ring and P. Schuck, *The Nuclear Many-Body Problem* (Springer, 1980).
- [4] P. Bonche, S. Koonin, and J. W. Negele, *Phys. Rev. C* **13**, 1226 (1976).
- [5] J. Maruhn, P.-G. Reinhard, P. Stevenson, and A. Umar, *Computer Physics Communications* **185**, 2195 (2014).
- [6] J. Dobaczewski and J. Dudek, *Phys. Rev. C* **52**, 1827 (1995).
- [7] J. Dobaczewski and J. Dudek, *Computer Physics Communications* **102**, 166 (1997).
- [8] J. Dobaczewski and J. Dudek, *Computer Physics Communications* **102**, 183 (1997).
- [9] J. Dobaczewski and J. Dudek, *Computer Physics Communications* **131**, 164 (2000).
- [10] J. Dobaczewski and P. Olbratowski, *Computer Physics Communications* **158**, 158 (2004).
- [11] J. Dobaczewski and P. Olbratowski, *Computer Physics Communications* **167**, 214 (2005).
- [12] J. Dobaczewski, W. Satuła, B. Carlsson, J. Engel, P. Olbratowski, P. Powalowski, M. Sadziak, J. Sarich, N. Schunck, A. Staszczak, M. Stoitsov, M. Zalewski, and H. Zduńczuk, *Computer Physics Communications* **180**, 2361 (2009).
- [13] N. Schunck, J. Dobaczewski, J. McDonnell, W. Satuła, J. Sheikh, A. Staszczak, M. Stoitsov, and P. Toivanen, *Computer Physics Communications* **183**, 166 (2012).
- [14] N. Schunck, J. Dobaczewski, W. Satuła, P. Baczyk, J. Dudek, Y. Gao, M. Konieczka, K. Sato, Y. Shi, X. Wang, and T. Werner, *Computer Physics Communications* **216**, 145 (2017).
- [15] M. Stoitsov, J. Dobaczewski, W. Nazarewicz, and P. Ring, *Computer Physics Communications* **167**, 43 (2005).
- [16] M. Stoitsov, N. Schunck, M. Kortelainen, N. Michel, H. Nam, E. Olsen, J. Sarich, and S. Wild, *Computer Physics Communications* **184**, 1592 (2013).
- [17] A. Bulgac and M. M. Forbes, *Phys. Rev. C* **87**, 051301 (2013).
- [18] P. Bonche, H. Flocard, P. Heenen, S. Krieger, and M. Weiss, *Nuclear Physics A* **443**, 39 (1985).
- [19] B. Gall, P. Bonche, J. Dobaczewski, H. Flocard, and P.-H. Heenen, *Z. Phys. A* **348**, 183 (1994).
- [20] J. Terasaki, P.-H. Heenen, H. Flocard, and P. Bonche, *Nuclear Physics A* **600**, 371 (1996).
- [21] M. Yamagami, K. Matsuyanagi, and M. Matsuo, *Nucl. Phys. A* **693** (2001) 579.
- [22] E. Terán, V. E. Oberacker, and A. S. Umar, *Phys. Rev. C* **67**, 064314 (2003).
- [23] V. E. Oberacker, A. S. Umar, E. Terán, and A. Blazkiewicz, *Phys. Rev. C* **68**, 064302 (2003).
- [24] N. Tajima, *Phys. Rev. C* **69**, 034305 (2004).
- [25] J. C. Pei, M. V. Stoitsov, G. I. Fann, W. Nazarewicz, N. Schunck, and F. R. Xu, *Phys. Rev. C* **78**, 064306 (2008).
- [26] J. C. Pei, G. I. Fann, R. J. Harrison, W. Nazarewicz, Y. Shi, and S. Thornton, *Phys. Rev. C* **90**, 024317 (2014).
- [27] H. Oba and M. Matsuo, *Phys. Rev. C* **80**, 024301 (2009).

- [28] Y. Zhang, M. Matsuo, and J. Meng, *Phys. Rev. C* **83**, 054301 (2011).
- [29] Y. Zhang, M. Matsuo, and J. Meng, *Phys. Rev. C* **86**, 054318 (2012).
- [30] W. Ryssens, V. Hellemans, M. Bender, and P.-H. Heenen, *Computer Physics Communications* **187**, 175 (2015).
- [31] W. Ryssens, P.-H. Heenen, and M. Bender, *Phys. Rev. C* **92**, 064318 (2015).
- [32] S. Jin, A. Bulgac, K. Roche, and G. Wlazłowski, *Phys. Rev. C* **95**, 044302 (2017).
- [33] B. Schuetrumpf and W. Nazarewicz, *Phys. Rev. C* **92**, 045806 (2015).
- [34] B. Schuetrumpf, W. Nazarewicz, and P.-G. Reinhard, *Phys. Rev. C* **93**, 054304 (2016).
- [35] M. Afibuzzaman, B. Schuetrumpf, and H. M. Aktulga, *Computer Physics Communications* **223**, 34 (2018).
- [36] K. Bennaceur and J. Dobaczewski, *Computer Physics Communications* **168**, 96 (2005).
- [37] V. Blum, G. Lauritsch, J. Maruhn, and P.-G. Reinhard, *Journal of Computational Physics* **100**, 364 (1992).
- [38] D. Vautherin and D. M. Brink, *Phys. Rev. C* **5**, 626 (1972).
- [39] Y. Engel, D. Brink, K. Goeke, S. Krieger, and D. Vautherin, *Nuclear Physics A* **249**, 215 (1975).
- [40] E. Perlińska, S. G. Rohoziński, J. Dobaczewski, and W. Nazarewicz, *Phys. Rev. C* **69**, 014316 (2004).
- [41] J. Maruhn, P.-G. Reinhard, P. Stevenson, and A. Umar, *Computer Physics Communications* **185**, 2195 (2014).
- [42] P. Goddard, P. Stevenson, and A. Rios, *Phys. Rev. C* **92**, 054610 (2015).
- [43] M. Abramowitz and I. A. Stegun, *Handbook of Mathematical Functions* (Dover, New York, 1965).
- [44] P. Bonche, H. Flocard, and P. Heenen, *Computer Physics Communications* **171**, 49 (2005).
- [45] S. S. M. Wong, *Computational Methods in Physics and Engineering* (World Scientific, 1997).
- [46] https://en.wikipedia.org/wiki/Trilinear_interpolation.
- [47] K. Davies, H. Flocard, S. Krieger, and M. Weiss, *Nuclear Physics A* **342**, 111 (1980).
- [48] J. Dobaczewski and W. Nazarewicz, in *50 Years of Nuclear BCS*, edited by R. A. Broglia and V. Zelevinski (World Scientific, Singapore, 2012), pp. 40-60.